2-Carboxyethylgermanium sesquioxide as a promising anode material for Li-ion batteries

Evgeniya A Saverina, Roman R Kapaev, Pavel V Stishenko, Alexey S Galushko, Victoriya A Balycheva, Valentine P Ananikov, Mikhail P Egorov, Viatcheslav V Jouikov, Pavel A Troshin, Mikhail A Syroeshkin

FULL PAPER WILEY-VCH

2-Carboxyethylgermanium sesquioxide as a promising anode material for Li-ion batteries

Evgeniya A. Saverina,[a,b] Roman R. Kapaev,[c,d] Pavel V. Stishenko,[e] Alexey S. Galushko,[a] Victoriya A. Balycheva,[a,f] Valentine P. Ananikov,[a] Mikhail P. Egorov,[a] Viatcheslav V. Jouikov, [b] Pavel A. Troshin*[c,d], and Mikhail A. Syroeshkin*[a]

[a] E. A. Saverina, A. S. Galushko, V. A. Balycheva, Prof. Dr. V. P. Ananikov, Prof. Dr. M. P. Egorov, Dr. M. A. Syroeshkin
N. D. Zelinsky Institute of Organic Chemistry
Leninsky prosp. 47, 119991 Moscow (Russia)
E-mail: syroeshkin@ioc.ac.ru
[b] E. A. Saverina, Prof. Dr. V. V. Jouikov
CNRS, ISCR (Institut des Sciences Chimiques de Rennes)
University of Rennes
UMR 6226, F-35000 Rennes, France
E-mail: vjouikov@univ-rennes1.fr
[c] R. R. Kapaev, Prof. Dr. P. A. Troshin
Skolkovo Institute of Science and Technology
st. Nobel, 3, 121205 Moscow (Russia)
E-mail: troshin2003@inbox.ru
[d] R. R. Kapaev, Prof. Dr. P. A. Troshin
Institute for Problems of Chemical Physics RAS
Academician Semenov avenue 1, 142432 Chernogolovka, (Russia)
[e] Dr. P. V. Stishenko
Department of Chemical Engineering
Omsk State Technical University
Mira prosp. 11, 644050, Omsk (Russia)
[f] V. A. Balycheva
Dmitry Mendeleev University of Chemical Technology of Russia
Miusskaya sq., 9, 125047 Moscow (Russia)

Supporting information for this article is given via a link at the end of the document.((Please delete this text if not appropriate))

Abstract: Various forms of germanium, and germanium-containing compounds and materials are actively investigated as energy-intensive alternatives to graphite in the anodes of lithium-ion batteries. The most accessible form – germanium dioxide – has the structure of a 3D polymer, which accounts for its rapid destruction during cycling, and requires the development of further approaches to the production of nanomaterials and various composites based on it. For the first time, we propose here the strategy of using Ge sesquioxide $[O_{1.5}GeCH_2CH_2CO_2H]_n$ (2-carboxyethylgermanium sesquioxide, 2-CEGS), in lieu of GeO_2, as a promising, energy-intensive, and stable new source system for building lithium-ion anodes. Due to the presence of the organic substituent, the formed polymer has a 1D or a 2D space organization, which facilitates the reversible penetration of lithium into its structure. 2-Carboxyethylgermanium sesquioxide is common and commercially available, completely safe and non-toxic, insoluble in organic solvents (which is important for batteries use) but soluble in water (which is convenient for manufacturing diverse materials from it). This paper reports on preparing its micro- (flower-shaped agglomerates of ~1 μm thick plates) and nano-forms (needle-shaped 2-CEGS nanoparticles of ~500 × (50-80) nm) using common methods available in laboratory and industry such as vacuum and freeze-drying of aqueous solutions of 2-CEGS. The lithium half-cells anodes based on 2-CEGS show a capacity of ~400 mA h g^{-1} for microforms and up to 700 mA h g^{-1} for nano-forms, which is almost two times higher than the maximal theoretical capacity of graphite. These anodes are stable during the cycling at various rates. The results of DFT simulation suggest that Li atoms form the stable Li_2O with the oxygen atoms of 2-CEGS, and actual charge-discharge cycle involves deoxygenated GeC_3H_5 molecules. Thus, C_3 chains loosen the anode structure compared to pure Ge improving its ability to accommodate Li ions.

Introduction

The importance of lithium-ion batteries (LIBs) in the development of a wide variety of modern electricity-driven devices, from microelectronics to electric vehicles and drones, is extremely high. In 2019, their invention was recognized by a Nobel Prize in Chemistry.[1] The energy efficiency of LIBs stems from the relative compactness of the lithium cation as a smallest positive charge carrier and from the ability of electrode materials to retain and bind the maximal amount of lithium involved in the redox scheme during charging and discharging the battery. Graphite, the ubiquitous LIBs anode material, has a theoretical limit of capacity of 372 mA h g^{-1} corresponding to the formation of LiC_6.[2] A large number of alternative materials with a higher theoretical capacity have been proposed,[3] in particular, anodes based on carbon analogs of group 14 of the Periodic Table — silicon,[4] germanium [5,6] and tin,[7] as well as on their compounds, e.g. oxides,[8] sulfides,[9] phosphides,[10] tellurides [11] etc.

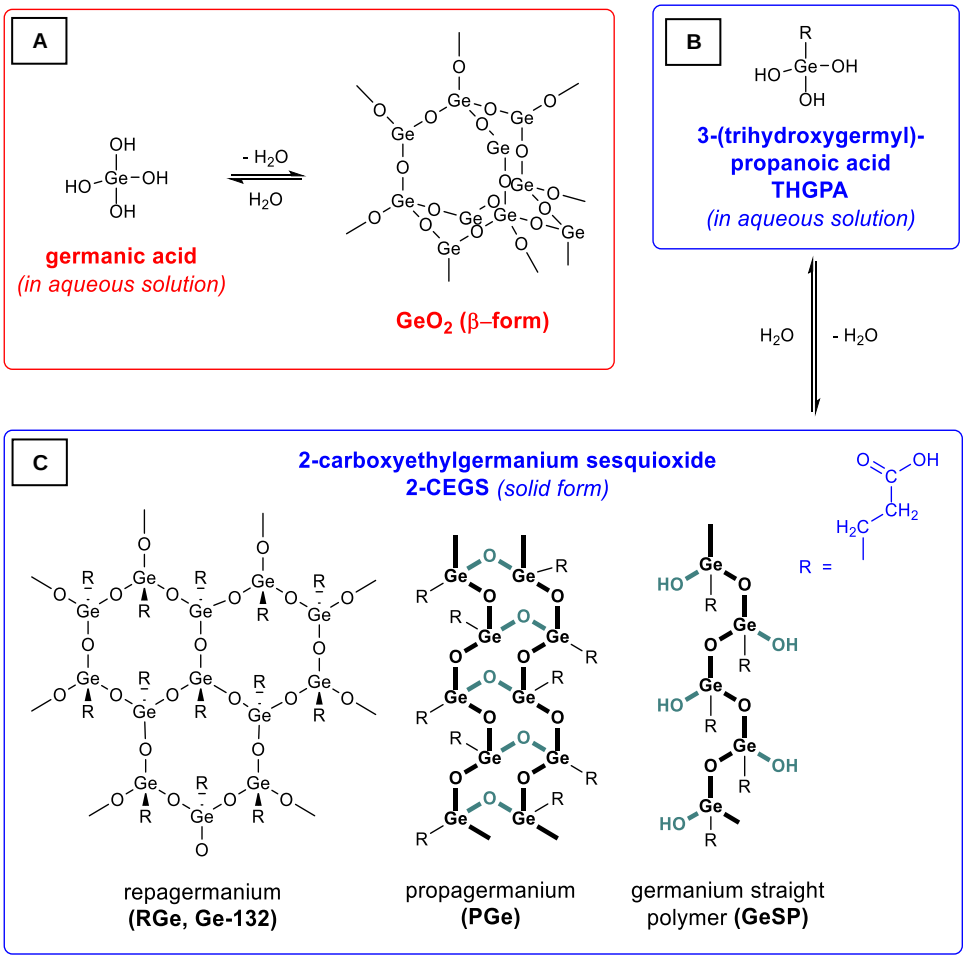

Figure 1. A) Germanium dioxide in an aqueous solution (germanic acid) and in the absence of water (3D polymer, β-form is presented). B) 2-Carboxyethyl germanium sesquioxide (2-CEGS) in aqueous solution (3-(trihydroxygermyl) propanoic acid); C) its various structural forms resulting from dehydration – repagermanium (2D polymer), propagermanium and germanium straight polymer (linear polymers).

One of the main problems on the way of producing an "ideal" anode material is that the parameters determining the performance of a battery - energy intensity and a maximum number of charge-discharge cycles – are intrinsically conflicting. On the one hand, the material must be able to bind a maximal amount of lithium, and on the other hand, lithium intercalation leads to a large volume expansion and its rapid deterioration. Remarkably, the first attempt to use germanium dioxide as an anode showed an excellent capacity of 740 mA h g^{-1} in the first cycle, yet collapsing down to 220 mA h g^{-1} by the 10th cycle.[12] As reflected in a number of recent works [13], current approaches use GeO_2 in its nano-forms and various composite materials allowing one to overcome the problem of dimensional stability of anodes and their low cycling ability.

The obvious requirement of new approaches and methods of obtaining new energy-intensive and efficient materials for batteries is their simplicity and accessibility, including for scaling up. Our attention was drawn to the fact that a similar problem relevant to the conversion of germanium dioxide was solved in medicine.

Germanium is a physiologically important microelement, but its dioxide is physiologically relatively inert,[14] which is associated with the stability of its three-dimensional polymer structure (Fig. 1a).[15] At the same time, occupying one valence of Ge with an organic substituent, the carboxyethyl group, prevents the resulting product from packing into dense 3D forms and renders its structure more susceptible to penetration of water molecules and consequently to hydrolysis (Fig. 1b). What if this principle also works with lithium cations?

First reported by Mironov more than half a century ago,[16] 2-carboxyethylgermanium sesquioxide (2-CEGS) was very intensively studied as a biologically active agent, especially by Asai and other Japanese scientists.[17] Currently, this water-soluble organic compound of germanium is the most widespread, commercially available Ge-containing drug. Under the designation of Ge-132, repagermanium and others, it was investigated as having antioxidant,[18] antitumor,[19] anti-hepatitis,[20] and anti-inflammatory[21] properties. In water, hydrolyzed Ge-132 loses its antioxidant properties, but is effective as an anti-oxidant in an anhydrous environment [22]. This behavior formally resembles the working conditions of the anode material in a lithium-ion battery, where the anode acts as a reducing agent ("antioxidant") with respect to lithium cations.

This work aims to study 2-CEGS as a potential energy-intensive and cyclically stable organic analogue of germanium dioxide in the anodes of lithium-ion batteries. As far as we know, it was not considered in such a capacity previously (and generally has not been studied in materials science).

Results and Discussion

Preparation of materials. 3-(trihydroxygermyl) propanoic acid (THGPA) was prepared from germanium dioxide using the known procedure (Scheme 1).[23]

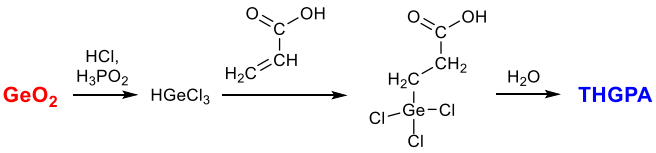

Scheme 1. Synthesis of 3-(trihydroxygermyl) propanoic acid.

At the final stage, the aqueous solution contains 3-(trihydroxygermyl) propanoic acid (THGPA), and the absence of other forms can be confirmed by ^{1}H and ^{13}C NMR spectroscopy (Fig. S10-S11). This acid is a structural analogue of germanic acid, in which one of the hydroxyl groups is replaced by a bulky and hydrophilic organic substituent (Fig. 1). During dehydration, the presence of the latter prevents the packaging into stable 3D polymer forms, and thus contributes to its much higher solubility in water (which accounts for the use of this material in the biomedical fields as a water-soluble compound of germanium [24]).It was logical to assume that the morphology of the sample at micro- and nanoscale, as well as chemical composition of the polymer will influence the target properties of the obtained material when used in LIBs, so the appropriate study was undertaken in order to elucidate this point.

Evaporation of an aqueous THGPA solution under vacuum leads to a dense white powder consisting, according to scanning electron microscopy (SEM), of fine flower-shaped agglomerates 50-70 μm in size, consisting of irregular platelets 10-20 μm in diameter and ca. 1 μm thick (Fig. 3, left). Slow crystallization of this sample over a period from several days to several weeks leads to a crystalline product whose X-ray diffraction pattern is identical to of the 2D polymer form of 2-CEGS (RGe, Fig. 1) described by Tsutsui et al. [25]

XRD analysis of the sample obtained by vacuum evaporation reveals the presence of the signals corresponding to RGe and to other phases. Fig. 2 shows the corresponding experimental diffractogram in comparison with the calculated one.

The X-ray diffraction parameters of two more ordered phases of 2-CEGS are known from the literature: the linear propagermanium polymer (PGe) consisting of two interwoven sesquioxide filaments, and the germanium straight polymer (GeSP), formed by a single strand of incompletely dehydrated (retaining part of the hydroxyl groups) polymer (Fig. 1). Their model diffraction patterns are constructed in Fig. 2 (d, e) using the data of X-ray diffraction analysis of these forms [25-26]. The sample obtained by vacuum evaporation of THGPA contains all the structural motifs. Thus, despite the dense and relatively ordered morphology, the chemical structure of the polymer compound is relatively “loose”, which is generally favorable given its intended purpose.

The decrease in the particle size of 2-CEGS obtained after the removal of water, up to the nanoscale, could potentially improve the quality of the material involved in the reversible heterogeneous process. Therefore, we investigated the possibility replacing direct vacuum evaporation of the THGPA solution in favor of its freeze-drying.

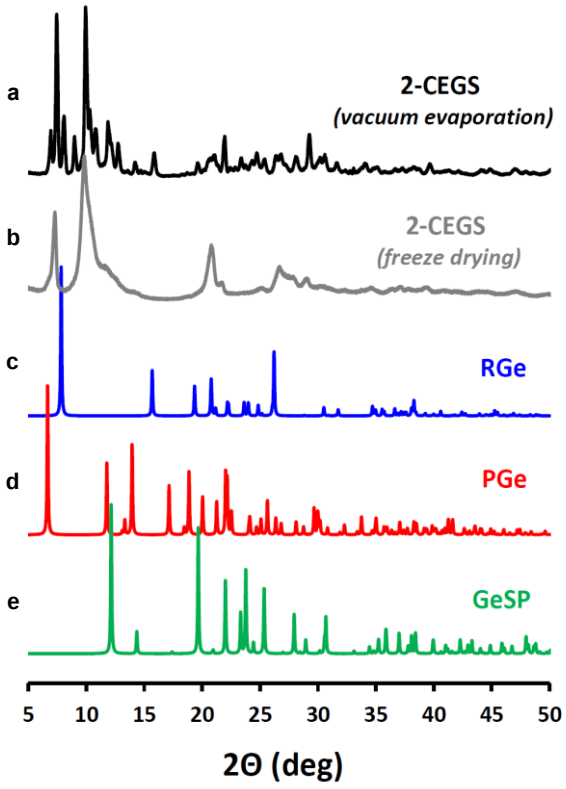

Figure 2. XRD data of 2-CEGS samples obtained by vacuum evaporation (a) and freeze-drying (b) from 0.1 mg mL^{-1} aqueous solution in comparison with model X-ray diffraction patterns of RGe (c, from [25]), PGe (d) and GeSP (e, from [26]).

This method of water removal is technically simple and widespread in laboratory and industrial practice;[27] the method consists in freezing the solution and subsequent sublimation of water under vacuum (Fig. 3, center/bottom) and allows us to get the smallest particles. Fig. 3 (center) features the SEM images of a sample 2-CEGS obtained by freeze-drying an aqueous solution of THGPA (1 mg mL^{-1}). Not only a decrease in particle size (about one order of magnitude) but also a qualitative change in the morphology are observed. In contrast to the lamellar product obtained by vacuum drying, the morphology of the freeze-dried sample is needle-shaped with particles 1.5-2 μm long and ~200 nm thick.

When the concentration of the THGPA solution is decreased to 0.1 mg mL^{-1}, the needles of 2-CEGS nanoparticles become even smaller, with a thickness down to 50 nm and a length of ~500 nm (Fig. 3, right; Fig. S7). This sample is also very different from the sample obtained by vacuum evaporation in appearance; now it is very light so that its loose and fluffy particles move in the air. It would also be interesting to see if there are differences in the biological activity of such samples. The X-ray diffraction pattern of the obtained sample (Fig. 2b) shows, that as in the case of the sample obtained by vacuum evaporation, this material contains signals characteristic of RGe, PGe and GeSP. However, the signals are significantly broadened, which is typical for nanoscale samples in which the ordered arrangement of atoms at long distances in crystallites is limited by their small size. Freeze-drying of a 0.5 mg mL^{-1} aqueous solution of 2-CEGS also allows the formation of nanoscale material.

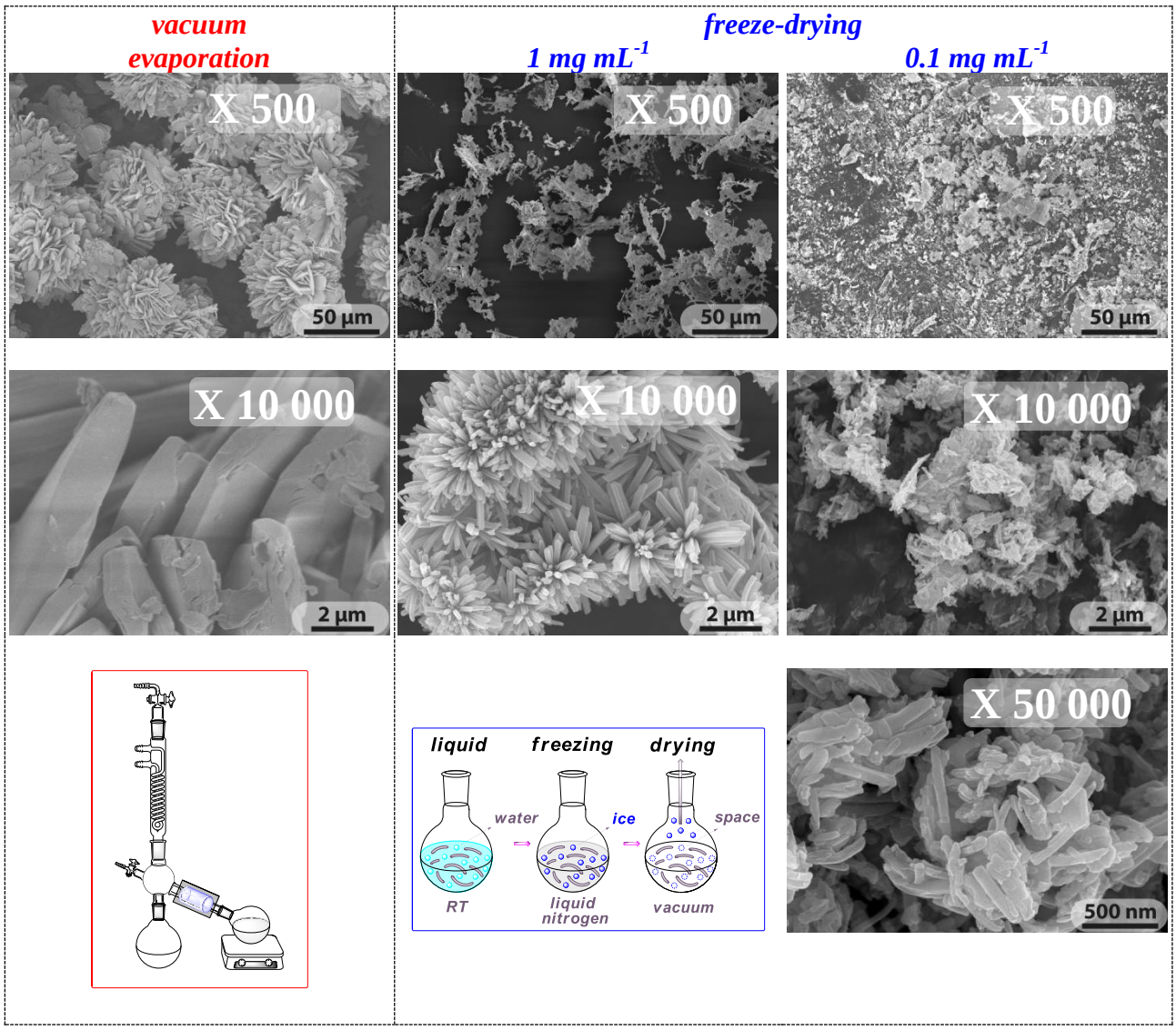

Figure 3. Scanning electron microscopy (SEM) images of 2-CEGS samples obtained by vacuum evaporation (left) and freeze-drying its 1 mg mL^{-1} (center) and 0.1 mg mL^{-1} (right) aqueous solutions (see also SI for large images).

We also investigated the possibility of obtaining nanosized GeO_2 by freeze drying. For this, we prepared a 0.1 mg mL^{-1} water solution of GeO_2 and subjected it to freeze-drying. However, the resulting material is micro-sized particles collected in circular-shaped agglomerates and, therefore, was not investigated as a potential material for anodes of lithium-ion batteries (Fig. S8).

In summary, the use of common practical methods of vacuum evaporation and freeze-drying allows us to obtain micro- and nano-forms of 2-CEGS having a soft polymer structure. In this study of 2-CEGS as anode material in lithium-ion cells, we used microsamples obtained by vacuum evaporation and nanosamples obtained by freeze-drying 0.1 mg mL^{-1} THGPA aqueous solutions.

Battery testing. The freeze-drying nanosized 2-CEGS samples were tested as an anode material for lithium-ion batteries. To make the electrode conductive, it was mixed with Super P carbon black. Within 0.01–3.0 V vs. Li^+/Li potential range, reversible capacity of 2-CEGS/C composite was found to be 659 mA h g^{-1} at 20 mA g^{-1} (Fig. 4). At a relatively high current density of 500 mA g^{-1}, 274 mA h g^{-1} were delivered. The average delithiation potential at 20 mA g^{-1} was 0.7 V vs. Li^+/Li, which is a typical value for alloying anodes, such as Ge, Sn, Bi, etc.[3; 28] A cell made in a similar way based on a micro-sized sample 2-CEGS (obtained by vacuum evaporation) allows reaching a capacity of up to 400 mA h g^{-1} (Fig. S9).

Charge-discharge curves and cyclic voltammetry profiles were characteristic of germanium, [6] indicating irreversible reduction of 2-CEGS to Ge during the initial cycles. This process apparently caused an activation effect, i.e. growth of the specific capacity during the first cycles. This activation results from the increasing conductivity of the material due to transformation of the insulating 2-CEGS to metallic Ge. Similar behavior was previously observed for other materials whose conductivity grows upon the first discharge. [29]

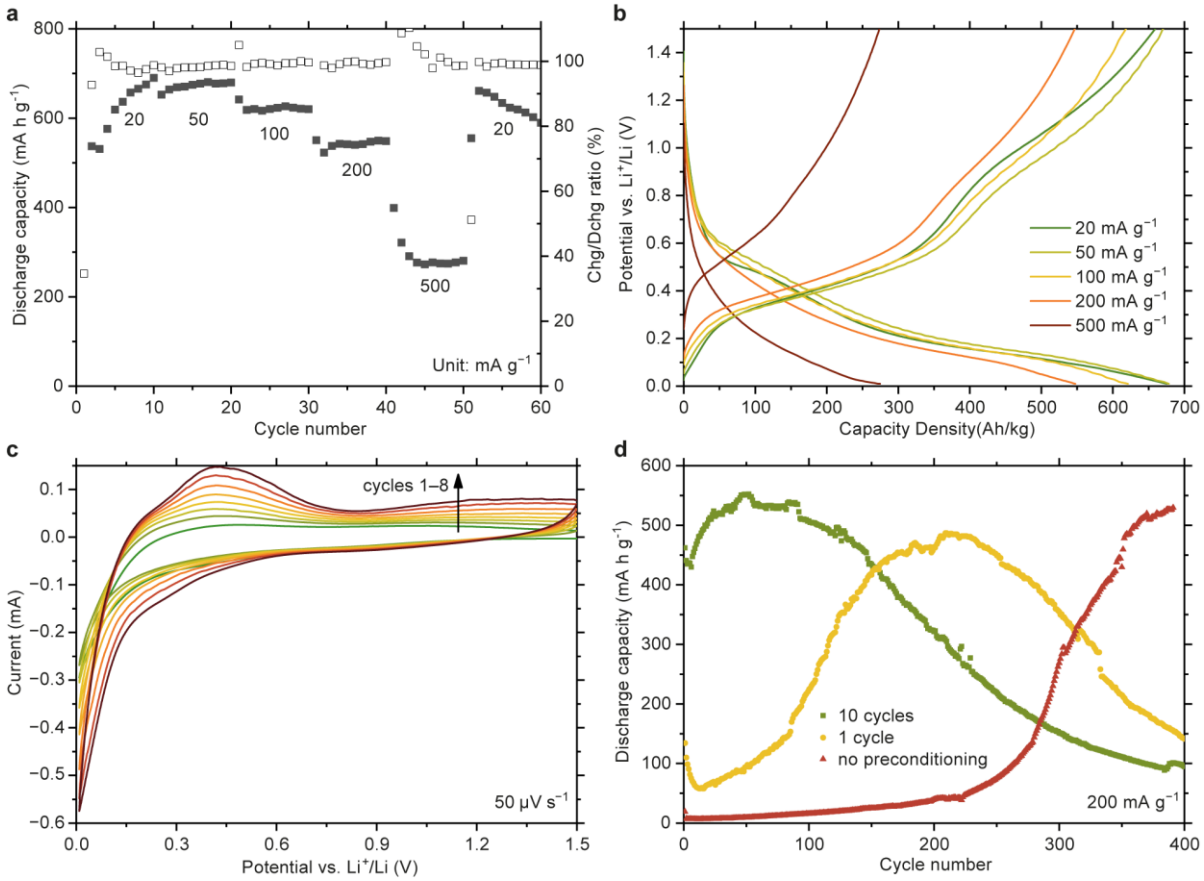

Figure 4. Electrochemical behavior of nanosized 2-CEGS obtained by freeze-drying 0.1 mg mL^{-1} aqueous solutions: (a) specific capacity and coulombic efficiency at different current densities; (b) charge-discharge profiles at different current densities; (c) cyclic voltammograms recorded at 50 μV s^{-1} scan rate at different cycle numbers; (d) cycling stability at 200 mA g^{-1} with different pre-conditioning options.

The activation phenomenon was especially pronounced at a relatively high current density of 200 mA g^{-1} (Fig. 4d). Without pre-conditioning of the electrodes, the capacity was <100 mA h g^{-1} for the first ~250 cycles, and then it gradually increased to ~550 mA h g^{-1} by the 400th cycle. However, if the material was charged and discharged at 20 mA g^{-1} prior to cycling, the capacity reached its maximum after approximately 200 cycles.

Moreover, if ten pre-conditioning cycles at 20 mA g^{-1} were performed, the maximal capacity of ~550 mA h g^{-1} was reached already by the 50th cycle. This behavior indicates that kinetics of the irreversible transformation of 2-CEGS to Ge is much slower compared to alloying/dealloying of germanium. The possible reason for such slow kinetics is low conductivity of 2-CEGS, which hinders the electron transfer. After the activation, the material demonstrated moderate cycling stability, with ca. 80% capacity retention after 100 cycles and ca. 60% retention after 150 cycles.

We suppose that the electrochemical performance of 2-CEGS can be improved by tuning the electrode or electrolyte composition. The rate performance might be enhanced by preparing composites with graphene or carbon nanotubes [30]. This approach is especially useful for active materials with low electron conductivity and, therefore, will likely be promising for 2-CEGS. The cycling stability might be improved by tuning the binder, which would provide better structural integrity or/and more robust solid electrolyte interphase (SEI) [31-32]. Properties of the SEI, which is known to affect the electrochemical stability strongly, can also be regulated by modifying the electrolyte composition [32]. Overall, we believe that further investigation of 2-CEGS and similar compounds may pave a new avenue to the anodes with high capacity, decent cycling stability and high rate capabilities.

Mechanistic insights. In order to get mechanistic insights into the interaction of 2-CEGS with Li atoms, we employed density functional theory (DFT) simulations. The RGe (Fig. 1, lower left corner) structure formed during crystallization of 2-CEGS from an aqueous solution was used as a model. We optimized the geometry of several relevant phases of Li in RGe and in its derivatives looking for the geometries with the lowest internal energy. Particularly we considered a single RGe unit cell filled with up to 21 Li atoms, Li_2O unit cell and two C_3H_5Ge molecules remaining after Li atoms abstracted oxygen from RGe to form Li_2O.

Optimized Li-RGe structures show that in an empty RGe cell the most preferential site for Li atom is in the center of GeO ring (Fig. 5). The second and third Li atoms tend to absorb near the same ring and between the carboxyl groups. Li atom located near the carboxyl groups coordinates with the oxygens in a tetrahedral manner. Other Li atoms up to the seventh one, preferentially

locate near the Ge-O rings coordinating with Ge and O atoms. At the same time, adding Li atoms decreases the coordination of Ge atoms by oxygen and splits the RGe structure into $C_3H_5GeO_2$ units with Li_2O between them (Fig. 6). Further simulated annealing of Li_{14}-RGe and Li_{21}-RGe structures (Fig. 7) confirmed the tendency of Li atoms to surround the oxygen and to abstract it from Ge and then from the carbon atoms.

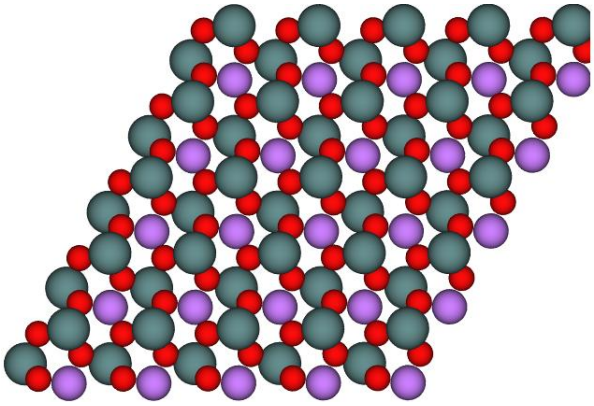

Figure 5. Li atoms (purple spheres) in Ge-O rings of RGe in case of one Li atom per RGe unit cell. Oxygen atoms - red spheres, germanium atoms - turquoise spheres. Top view, carboxyl chains are not shown for clarity.

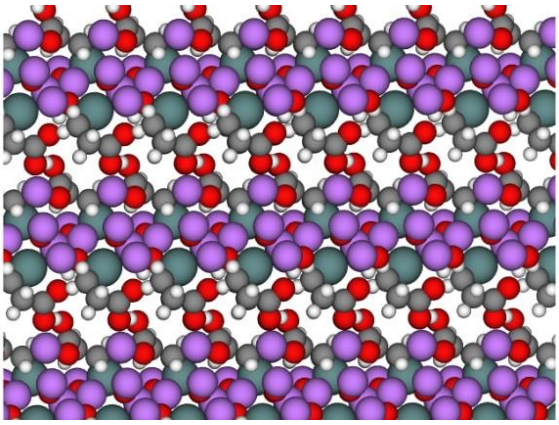

Figure 6. Side view of RGe-Li_7 structure. Colors as in Figure 5.

We suppose that lithium oxide Li_2O tend to crystallize into a solid phase. Oxygen removal from RGe unit cell leaves there two C_3H_5Ge molecules (Fig. 8, left). Energy optimizations have shown that the RGe unit cell with 14 Li atoms is less energetically favorable than the separated Li_2O and C_3H_5Ge structures with the same chemical composition.

Annealing simulations demonstrated that oxygen atoms from the Ge-O ring are used to form Li_2O before the oxygen from the carboxylic acid groups. So we also optimized the structures of partially deoxygenated RGe with the oxygen retained the in carboxylic groups ($C_3H_5GeO_4$). The $C_3H_5GeO_4$ structure is shown in Fig. 8 (center). The same structure with a single Li atom in the vicinity of oxygen atoms is also shown in Fig. 8 (right). The resulting compositions of $3Li_2O + 2C_3H_5GeO_4$ and $3Li_2O + Li\text{-}2C_3H_5GeO_4$ turned out to be more energetically favorable compared to the corresponding concurrent structures Li_6-RGe and Li_7-RGe.

Assuming that all oxygen atoms from RGe could be converted into Li_2O, we computed the phases with several Li atoms in deoxygenated RGe of the general formulae $Li_x\text{-}2C_3H_5Ge$ (where x = 0, 1, 4 or 7 corresponding, respectively, to 14, 15, 18 or 21 Li atoms per RGe unit cell and considering that the Li atoms all exist as Li_2O phase, Fig. 9). The obtained phases turned out to be more energetically favorable than the corresponding Li-RGe phases with the equivalent number of Li atoms. In the $Li_7\text{-}2C_3H_5Ge$ structure obtained from the simulation, the bonds between the Ge atoms and the carbon chains tend to be elongated and are probably broken; however, this can be an artifact of the simulated annealing, so we cannot say for sure if this bond breaking is kinetically realizable under the conditions of exploitation of Li batteries.

The layers of Ge atoms in the obtained structures are separated by the layers of C_3 carbon chains while Li atoms are distributed in this structure without a clear location preference. Probably, more stable structures with large unit cells also exist but at this point we were unable to find them with the available computational resources.

Following the established approach to DFT studies of Li-ion batteries, [33] the phase formation energies were calculated and the convex hull was plotted for the intermediate Li compositions (Fig. 10). Only phases that correspond to points on the convex hull are thermodynamically stable. For each phase in a convex hull interior, a composition of nearby phases on the convex hull boundary with smaller energy exists. The convex hull of up to 14 Li atoms is fully constituted with the phases where all Li atoms are converted into Li_2O form. Even the $3Li_2O + Li\text{-}2C_3H_5GeO_4$ phase is less favorable than the corresponding composition of neighboring phases ($3Li_2O + C_3H_5GeO_4$ and $7Li_2O + 2C_3H_5Ge$). Therefore, various Li concentrations are constituted by compositions of RGe, Li_2O and C_3H_5Ge phases.

Overall, the complexity of the physicochemical processes occurring during lithiation of 2-CEGS and the stepwise formation of metallic germanium also explains the activation phenomenon noted during the electrochemical studies.

Experimental Section

Reagents and materials. 2-CEGS has been prepared from $HGeCl_3$ and acrylic acid according to ref. [23]. $HGeCl_3$ has been prepared from GeO_2 (Germanium and Applications Ltd, DG-B, TY 1774-001-95961127-2010). NMR data for 2-CEGS: ^1H NMR (300 MHz, D_2O, δ, ppm): 1.58 (t, 2H, CH_2, J = 7.5 Hz), 2.58 (t, 2H, CH_2, J = 7.5 Hz); ^{13}C NMR (150 MHz, D_2O, δ, ppm): 12.49 (CH_2), 26.93 (CH_2), 177.90 (COOH), which can be compared with published data. [19c] Ethylene carbonate (EC) and dimethyl carbonate (DMC) were dried by standard methods.[34]

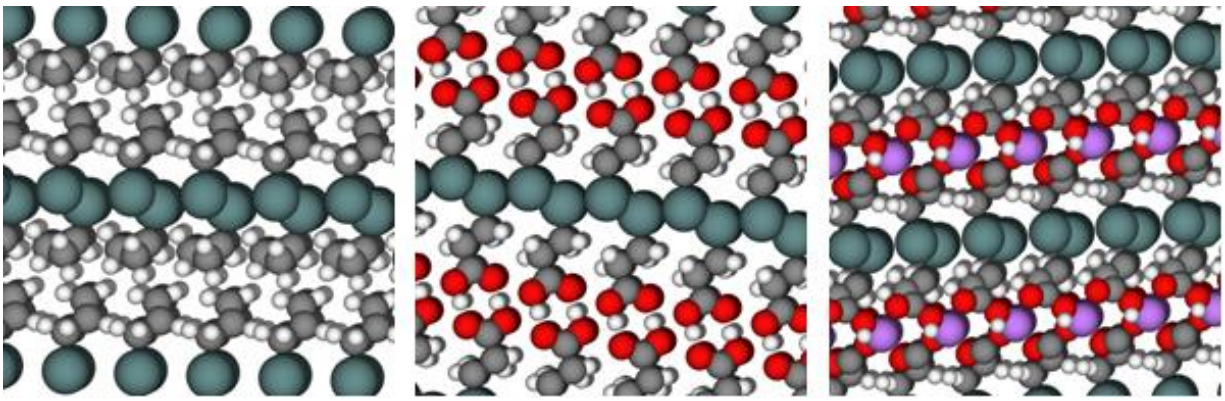

Figure 8. Deoxygenated RGe structures: completely deoxygenated C_3H_5Ge (left), partially deoxygenated $C_3H_5GeO_4$ (center) and $C_3H_5GeO_4$ with one Li atom (right). Colors as in Figure 5.

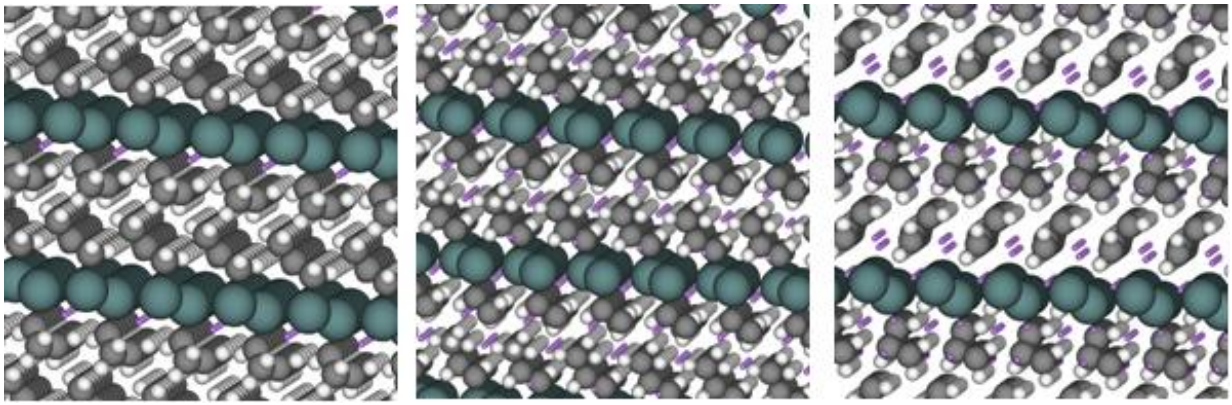

Figure 9. Li atoms in deoxygenated RGe. Li_x-$2C_3H_5Ge$ where x = 1 (left), x = 4 (center) and x = 7 (right). Colors as in Figure 5.

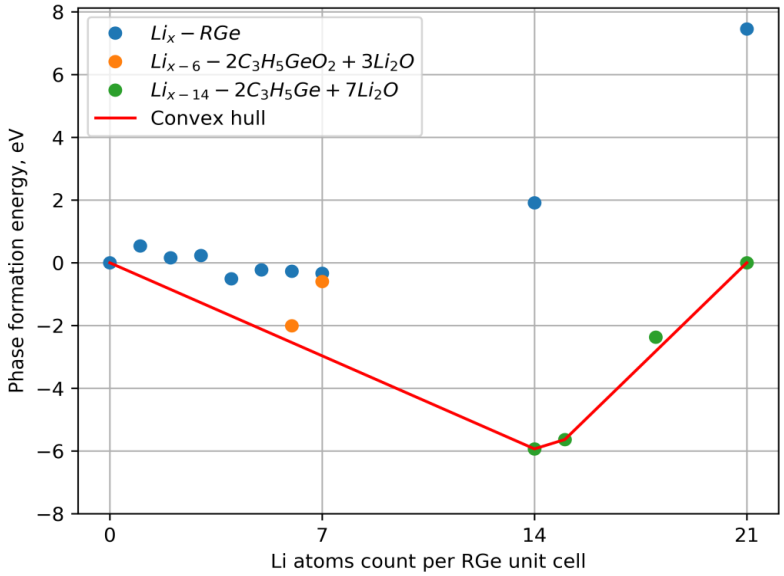

Figure 10. Phase formation energy diagram with convex hull. Blue dots - phases of Li in RGe, orange dots - phases of Li in partially deoxygenated RGe with oxygen transformed into Li_2O phase, green dots - phases of Li in completely deoxygenated RGe

Freeze-drying of the samples was performed using a Christ Alpha 1-2 Freeze Dryer.

NMR spectra were recorded on Bruker AV300 (^{1}H) and AV600 (^{13}C) spectrometers at ambient temperature.

SEM measurement. The observations were carried out using a field emission scanning electron microscope Hitachi SU8000 (FE-SEM). A thin 10 nm-thick Au/Pd (60/40) layer was deposited by magnetron sputtering on non-conductive samples [35] The morphology of the samples was studied taking into account the possible effect of the deposited conductive layer on the surface [35]. Images were obtained in the mode of secondary electrons at a working distance of 8-10 mm and at an accelerating voltage of 2-10 kV.

X-ray experiments. Powder X-ray diffraction patterns were recorded using a Bruker D8 Advance X-ray diffractometer (CuKα, 40 kV, 40 mA, Ni-filter, LYNXEYE detector, reflection geometry). The single crystal X-Ray diffraction analysis was performed on a Bruker SMART APEX2 instrument.

Li-ion battery assembling and characterization. For preparing the electrodes, 2-CEGS, carbon black (Super P) and polyvinylidene fluoride (PVdF) were mixed in a weight ratio 6:3:1 in N-methylpyrrolidone, the resulting slurry was tape-casted onto a carbon-coated copper foil. The electrode was dried in air at 70 ˚C for 30 min, then vacuum-dried at 110 ˚C for 5 h, calendered at room temperature and vacuum-dried again at 110 ˚C for 5 h. The resulting electrode loading was ~1.5 mg cm^{-2}.
The electrodes were tested in CR2032-type coin cells assembled in an Ar-filled glovebox with oxygen and moisture levels below 1 ppm. Lithium foil was used as the anode, glass fiber was used as the separator, 1 M $LiPF_6$ in EC:DMC (1:1 v/v) was used as the electrolyte. The working electrodes were cycled galvanostatically in 0.01–1.5 V range. Specific capacities and current densities were calculated per combined mass of 2-CEGS and Super P. Coulombic efficiency was defined as the ratio between charge (demetalation) and discharge (metalation) capacities multiplied by 100%. Cyclic voltammograms were recorded at a scan rate of 50 μV s^{-1} in 0.01–1.5 V range.

DFT. Global optimization of such a complex system is extremely computationally expensive. Therefore, to get as close to optimal structures as possible we employed heuristics based on the following a priori ideas about the energy landscape of this system. First, Li atoms tend to coordinate in the vicinity of oxygen atoms, hence local optimization algorithms are unable to move Li atoms between spatially separated groups of oxygen atoms. Second, Li atoms tend to abstract oxygen from germanium oxides forming separate Li_2O and Ge phases.[36] Third, simulated annealing drives a complex system towards the energy minimum.
For RGe containing from 1 to 7 Li atoms per unit cell we conducted a series of local optimizations adding Li atoms one-by-one to the structures optimized in the previous step, starting from the empty RGe cell. The optimizations were conducted for two probable initial positions of a newly added Li atom: either in the Ge-O ring plane, or between the carboxyl groups. During the optimization, the newly added atom drifted in all cases towards nearby oxygen atoms and never from the initial position to another group of oxygen atoms. Therefore, we obtained the energies of locally optimized structures with various distribution of Li atoms. A complete table of these energies is provided in Supplementary Information (Table S1-S2). Further following this strategy for a larger number of Li atoms does not make sense due to distortion of the unit cell structure, oxygen groups with Li atoms cannot be reliably distinguished anymore.
Therefore, for a unit cell with a larger number of Li atoms, we simulated the annealing process using ab initio molecular dynamics in an NVT ensemble. The temperature during the simulations was decreased from 1500 K to 400 K with 100 K steps. At each temperature step, the system was simulated for 85 fs totaling to 1020 fs for the overall annealing simulation. Finally, local optimization was performed. This procedure was used for Li_{14}-RGe, Li_{21}-RGe, and for Li_x-2C_3H_5Ge (x = 0, 1, 4, 7) structures.
All optimizations, excluding Li_2O structure, were conducted for the unit cells with 2 Ge atoms, with 3×3×1 k-point grid. Local optimizations were conducted in two stages: at first stage a variable cell geometry optimization was employed within LDA DFT approximation; at second stage the geometry was optimized with a fixed unit cell using the revPBE[37] DFT approximation. Grimme D2 correction[38] has been applied in all computations. For local optimizations, 0.1 eV/A threshold was used for the convergence per atom. In all DFT computations the kinetic energy cut off was set at 1088 eV (80 Ry) and the energy cut off for plane wave basis of electron density was set 4 times larger. DFT computations were conducted with the Quantum Espresso suite.[39] Local optimizations and the simulated annealing procedure were implemented using the Atomic Simulation Environment (ASE).[40]

Conclusion

2-Carboxyethylgermanium sesquioxide can be effectively used as an anode material for lithium-ion batteries. The results obtained attest to a high capacity of such anodes, approaching 700 mA h g^{-1} (which is almost twice that of graphite) with good cycling. Its availability and convenient consumer-desired characteristics, such as solubility in water, stability and safety during storage and use, make it a promising material in this area. Thus, replacing one valence position in the 3D inorganic GeO_2 polymer with an organic substituent leads to a dramatic change in its structure, morphology, and physicochemical properties, primarily increasing the capacity of the inorganic framework to accommodate and host (or to interact with) small molecules. This seems to be a general and very convenient approach to creating germanium-based advanced materials. Given that the methods of production of organic sesquioxides are relatively simple and well developed, and that the palette of substituents allowing wide control of the product properties is, in principle, not limited, this area in our opinion certainly deserves further development in the field of lithium-ion batteries and in others fields of materials science.

Acknowledgements

Material preparation and characterization were supported at Zelinsky Institute of Organic Chemistry by Russian Science Foundation Grant 17-73-20281. Evaluation of electrochemical properties of the materials in batteries was supported by Russian Science Foundation at Skoltech (project No. 16-13-00111P). R.R.K. and P.A.T. also acknowledge general support from Russian Ministry of Science and Education received at IPCP RAS (project No. 0089-2019-0010). Electron microscopy and NMR spectra characterization were performed in the Department of Structural Studies of Zelinsky Institute of Organic Chemistry, Moscow. Powder and single crystal X-ray diffraction data were collected at the Centre for Collective Use of Kurnakov Institute of General and Inorganic Chemistry.

Keywords: Li-ion batteries • germanium • anode materials

[1] a) https://www.nobelprize.org/prizes/chemistry/2019/summary/ The Nobel Prize in Chemistry 2019; b) R.F. Service, *Science*, **2019**, *366*,

292, doi: 10.1126/science.366.6463.292; c) G. Armstrong, *Nature Chem.*, **2019**, *11*, 1076, doi: 10.1038/s41557-019-0386-7.

[2] J.-M. Tarascon, M. Armand, *Nature*, **2001**, *414*, 359, doi: 10.1038/35104644.

[3] J. Lu, Z. Chen, F. Pan, Y. Cui, K. Amine, *Electrochem. Energy Rev*., **2018**, *1*, 35, doi: 10.1007/s41918-018-0001-4.

[4] P. Li, G. Zhao, X. Zheng, X. Xu, C. Yao, W. Sun, S.X. Dou, *Energy Storage Materials*, **2018**, *15*, 422, doi: 10.1016/j.ensm.2018.07.014

[5] a) D. Kwon, J. Ryu, M. Shin, G. Song, D. Hong, K. S. Kim, S. Park, *J. Power Sources*, **2018**, *374*, 217, doi: 10.1016/j.jpowsour.2017.11.044; b) Y. Yang , S. Liu, X. Bian, J. Feng, Y. An, C. Yuan, *ACS Nano*., **2018**, *12*, 2900, doi:10.1021/acsnano.8b00426; c) B. Liu, A. Chen, R. Wang, T. Sun, J. Zhang, Y. Shu, J. Yang, C. Wang, Y. Yang, *J. Inorg. Organomet. Polym. Mater*., **2019**, *1*, doi: 10.1007/s10904-019-01201-4; d) K. Stokes, W. Boonen, H. Geaney, T. Kennedy, D. Borsa, K.M. Ryan, *ACS Appl. Mater. Interfaces*, **2019**, *11*, 19372, doi: 10.1021/acsami.9b03931; e) J. Doherty, S. Biswas, D. McNulty, C. Downing, S. Raha, C. O'Regan, A. Singha, C. O'Dwyer, J.D. Holmes, *Chem. Mater*., **2019**, *31*, 4016, doi: 10.1021/acs.chemmater.9b00475; f) J. Liu, J. Xu, Y. Chen, W. Sun, X. Zhou, J. Ke, Int. J. *Electrochem. Sci*., **2019**, *14*, 359, doi: 10.20964/2019.01.08; g) Y. Liu, X. Xu, X. Jiao, L. Guo, Z. Song, S. Xiong, J. Song, *Chem. Eng. J*., **2019**, *371*, 294, doi: 10.1016/j.cej.2019.04.068.

[6] E.A. Saverina, V. Sivasankaran, R.R. Kapaev, A.S. Galushko, V.P. Ananikov, M.P. Egorov, V.V. Jouikov, P.A. Troshin, M.A. Syroeshkin, *Green Chem*., **2020**, *22*, 359, doi: 10.1039/C9GC02348H.

[7] J. Wu, Z. Zhu, H. Zhang, H. Fu, H. Li, A. Wang, H. Zhang, *Sci Rep*., **2016**, *6*, 29356, doi: 10.1038/srep29356.

[8] W. Wei, J. Xu, M. Xu, S. Zhang, L. Guo, *Sci. China Chem*., **2018**, *61*, 515, doi: 10.1007/s11426-018-9244-0.

[9] Y. Wei, J. He, Q. Zhang, C. Liu, A. Wang, H. Li, T. Zhaia, *Mater. Chem. Front.*, **2017**, *1*, 1607, doi: 10.1039/C7QM00060J.

[10] a) S. Haghighat-Shishavan, M. Nazarian-Samani, M. Nazarian-Samani, H.-K. Roh, K.-Y. Chung, S.-H. Oh, B.-W. Cho, S. F. Kashani-Bozorg, K.-B. Kim, *ACS Appl. Mater. Interfaces*, **2019**, *11*, 32815, doi: 10.1021/acsami.9b05900; b) W. Li, X. Li, J. Yu, J. Liao, B. Zhao, L. Huang, A. Abdelhafiz, H. Zhang, J. - H. Wang, Z. Guo, M. Liu, *Nano Energy*, **2019**, *61*, 594, doi: 10.1016/j.nanoen.2019.04.080; c) X. Li, W. Li, P. Shen, L. Yang, Y. Li, Z. Shi, H. Zhang, *Ceram.Int.*, **2019**, *45*, 15711, doi: 10.1016/j.ceramint.2019.04.219.

[11] K.-H. Nam, G.-K. Sung, J.-H. Choi, J.-S. Youn, K.-J. Jeon, C.-M. Park, *J. Mater. Chem. A*, **2019**, *7*, 3278, doi: 10.1039/c8ta12094c.

[12] M.V. Reddy, G.V. Subba Rao, B.V.R. Chowdari, *Chem. Rev*., **2013**, *113*, 5364, doi: 10.1021/cr3001884.

[13] a) D. McNulty, H. Geaney, D. Buckley, C. O'Dwyer, *Nano Energy*., **2018**, *43*, 11, doi: 10.1016/j.nanoen.2017.11.007; b) H. Song, B. Zhao, S. Yan, K. Li, X. Xu, Y. Shi, *J. Nanoscience Nanotechnol*., **2017**, *17*, 12, 9036, doi: 10.1166/jnn.2017.13899; c) F. Pantò, Y. Fan, S. Stelitano, E. Fazio, S. Patanè, P. Frontera, P. Antonucci, N. Pinna, S. Santangelo, *Int. J. Hydrogen Energy*, **2017**, *42*, 28102, doi: 10.1016/j.ijhydene.2017.05.051; d) H. Song, B. Zhao, X. Xu, S. Yan, Y. Shi, *Mater. Sci. Eng.: B*., **2017**, *225*, 122, doi: 10.1016/j.mseb.2017.08.021; e) W. Zhang, H. Pang, W. Sun, L.-P. Lv, Y. Wang, *Electrochem. Comm*., **2017**, *84*, 80, doi: 10.1016/j.elecom.2017.09.019; f) J. Zhang, T. Yu, J. Chen, H. Liu, D. Su, Z. Tang, J. Xie, L. Chen, A. Yuan, Q. Kong, *Ceram. Int.*, **2018**, *44*, 1127, doi: 10.1016/j.ceramint.2017.10.069; g) F. Pantò, Y. Fan, S. Stelitano, E. Fazio, S. Patanè, P. Frontera, P. Antonucci, N. Pinna, S. Santangelo, *Adv. Functional Mater*., **2018**, *28*, 1800938, doi: 10.1002/adfm.201800938; h) S. Wang, X. Gu, L. Wang, C. Wu, Q. Liu, L. Zhao, Y. Xue, W. Li, Y. Rui, J. Xu, M. Ding, *J. Nanosci. Nanotechnol*., **2019**, *19*, 263, doi: 10.1166/jnn.2019.16455; i) S.-Y. Lim, W. Jang, S. Yun, W.-S. Yoon, J.-Y. Choi, D. Whanga, *Mater. Res. Bull*., **2019**, *110*, 24, doi: 10.1016/j.materresbull.2018.10.007.

[14] E. Lukevics, L. Ignatovich, *Biological activity of organogermanium compounds*, Ch. 23, in: Z. Rappoport (Ed.), *The Chemistry of Organic Germanium, Tin and Lead Compounds*, *vol. 2*, John Wiley & Sons, **2002**, pp. 1653-1683.

[15] a) E.N. Nikolaevskaya, A.V. Kansuzyan, G.E. Filonova, V.A. Zelenova, V.M. Pechennikov, I.V. Krylova, M.P. Egorov, V.V. Jouikov, M.A. Syroeshkin, *Eur. J. Inorg. Chem*., **2019**, *676*, doi: 10.1002/ejic.201801259; b) E.N. Nikolaevskaya, E.A. Saverina, A.A. Starikova, A. Farhati, M.A. Kiskin, M.A. Syroeshkin, M.P. Egorov, V.V. Jouikov, *Dalton Trans*., **2018**, *47*, 17127, doi: 10.1039/C8DT03397H; c) E.N. Nikolaevskaya, P.G. Shangin, A.A. Starikova, V.V. Jouikov, M.P. Egorov, M.A. Syroeshkin, *Inorg. Chim. Acta*, **2019**, *495*, 119007, doi: 10.1016/j.ica.2019.119007.

[16] V.F. Mironov, E.M. Berliner, T.K. Gar, *Russ. J. Gen. Chem*., **1967**, *37*, 911 (in rus: *Zhurnal Obshchei Khimii*, **1967**, *37*, 962).

[17] K. Asai, *The Miracle Cure: Organic Germanium*; Japan Publications, Inc.; New York, 1st edition, **1980**, 171 p.

[18] a) T. Wada, T. Hanyu, K. Nozaki, K. Kataoka, T. Kawatani, T. Asahi, N. Sawamura, *Biol. Pharm. Bull*., **2018**, *41*, 749; doi: 10.1248/bpb.b17-00949; b) T. Takeda, S. Doiyama, J. Azumi, Y. Shimada, Y. Tokuji, H. Yamaguchi, T. Nakamura, *Sci. Rep*., **2019**, *9*, 13637, doi: 10.1038/s41598-019-49883-7; c) Y. Liu, L. Hou, Q. Li, Z. Jiang, W. Gao, Y. Zhu, H. Zhang, *Environment. Technol.,* **2016**, *38*, 85, doi: 10.1080/09593330.2016.1186226.

[19] a) S. Kikuchi, K. Noguchi, K. Wakai, Y. Hamazaki, K. Tozawa, T. Jomori, H. Miwa, *Anticanc. Res*., **2019**, *39*, 4687, doi: 10.21873/anticanres.13651; b) K. Yumimoto, S. Sugiyama, K. Mimori, K. Nakayama, *Cancer Sci*., **2019**, *110*, 2090, doi: 10.1111/cas.14075; c) S.M. Ogwapit, *Bioscience Horizons*, **2011**, *4*, 128, doi: 10.1093/biohorizons/hzr015.

[20] C. Hirayama, H. Suzuki, M. Ito, M. Okumura, T. Oda, *J. Gastroenterol*., **2003**, *38*, 525, doi: 10.1007/s00535-003-1098-7.

[21] P. Mulder, A.M. Hoek, R. Kleemann, *PLOS ONE*, **2017**, *12*, e0169740, doi: 10.1371/journal.pone.0169740.

[22] a) A.A. Vishtorskaya, E.A. Saverina, V.M. Pechennikov, I.V. Krylova, A.V. Lalov, M.A. Syroeshkin, M.P. Egorov, V.V. Jouikov, *J. Organomet. Chem*., **2018**, *858*, 8, doi: 10.1016/j.jorganchem.2018.01.004; b) G.E. Filonova, E.N. Nikolaevskaya, A.V. Kansuzyan, I.V. Krylova, M.P. Egorov, V.V. Jouikov, M.A. Syroeshkin, *Eur. J. Org. Chem*., **2019**, 4128, doi: 10.1002/ejoc.201900331.

[23] N. Kakimoto, M. Akiba and T. Takada, *Synthesis*, **1985**, *272*.

[24] a) T. Nakamura, T. Takeda, Y. Tokuji, *Int. J. Vitam. Nutr. Res*., **2014**, *84*, 183, doi: 10.1024/0300-9831/a000205; b) C.C. Ho, Y.F. Chern, M.T. Lin, *Pharmacology*, **1990**, *41*, 286, doi: 10.1159/000138736.

[25] M. Tsutsui, N. Kakimoto, D.D. Axtell, H. Oikawa, K. Asai, *J. Am. Chem. Soc*., **1976**, *98*, 8287, doi: 10.1021/ja00441a081

[26] N. Mizuno, E. Nishibori, M. Oka, T. Jomori, M. Takata, T. Kumasaka, *J. Pharm. Sci*., **2015**, *104*, 2482, doi: 10.1002/jps.24486.

[27] J. Corver, *Innov. Pharm. Technol*., **2009**, *66*, http://iptonline.com/articles/public/IPT_29_p66non%20print.pdf

[28] W.-J. Zhang, *J. Power Sources* **2011**, 196, 13-24, https://doi.org/10.1016/j.jpowsour.2010.07.020.

[29] R.R. Kapaev, S. Olthof, I.S. Zhidkov, E.Z. Kurmaev, K.J. Stevenson, K. Meerholz, P.A. Troshin, *Chem. Mater*., **2019**, *31*, 5197, doi: 10.1021/acs.chemmater.9b01366.

[30] a) N. Patil, A. Aqil, F. Ouhib, S. Admassie, O. Inganäs, C. Jérôme, C. Detrembleur, *Adv Mater*., **2017**, 29, 1703373, https://doi.org/10.1002/adma.201703373; b) X. Wu, Y. Guo, J. Su, J. Xiong, Y. Zhang, L. Wan, *Adv. Energy Mater*., **2013**, 3, 1155-1160; c) Y. Huang, K. Li, J. Liu, X. Zhong, X. Duan, I. Shakirc, Y. Xu, *J. Mater. Chem. A,* **2017**, 5, 2710-2716, https://doi.org/10.1039/C6TA09754E; d) C. Li, Q. Deng, H. Tan, C. Wang, C. Fan, J. Pei, B. Cao, Z. Wang, J. Li, *ACS Appl. Mater. Interfaces,* **2017**, 9, 27414-27420, https://doi.org/10.1021/acsami.7b08974

[31] a) C. Bommier and X. Ji, *Small* **2018**, 14, 1703576, https://doi.org/10.1002/smll.201703576; b) T. Kwon, J. Choi, A. Coskun, *Chem. Soc. Rev*. **2018**, 47, 2145-2164, https://doi.org/10.1039/C7CS00858A

[32] a) S. Zhang, J. *Power Sources* **2006**, 162, 1379-1394, https://doi.org/10.1016/j.jpowsour.2006.07.074; b) M. Muñoz - Márquez, D. Saurel, J. Gómez - Cámer, M. Casas - Cabanas, E. Castillo - Martínez, T. Rojo, *Adv. Energy Mater*. **2017**, 7, 1700463, https://doi.org/10.1002/aenm.201700463; c) R. Kapaev, I. Zhidkov, E.

Kurmaev, K. Stevenson, P. Troshin, *J. Mater. Chem. A,* **2019**, 7, 22596-22603, https://doi.org/10.1039/C9TA06430C
[33] A. Urban, D.-H. Seo, G. Ceder, *Comp. Mat*., **2016**, *2*, 16002, doi: 10.1038/npjcompumats.2016.2.
[34] D.D. Perrin, W.L.F. Armarego, D.R. Perrin, Purification of Laboratory Chemicals, *Pergamon Press*, Oxford, **1980**.
[35] A.S. Kashin, V.P. Ananikov, *Russ. Chem. Bull. Int. Ed*. **2011**, *60*, 2602, doi: 10.1007/s11172-011-0399-x
[36] J. Wu, N. Luo, S. Huang, W. Yang, M. Wei, *J. Mater. Chem. A*, **2019**, 7, 4574, doi: 10.1039/C8TA12434E.
[37] Y. Zhang, W. Yang, *Phys. Rev. Lett.,* **1998**, *80*(4), 890–890, doi:10.1103/physrevlett.80.890
[38] S. Grimme, *J. Comput. Chem.,* **2006**, *27*(15), 1787–1799, doi:10.1002/jcc.20495
[39] P. Giannozzi et al., *J. Phys.: Condens. Matter*., **2009**, *21*, 395502, doi: 10.1088/0953-8984/21/39/395502.
[40] A.H. Larsen et al., *J. Phys.: Condens. Matter*., **2017**, *29*, 273002, doi: 10.1088/1361-648X/aa680e.

10.1002/cssc.202000852

WILEY-VCH

Entry for the Table of Contents

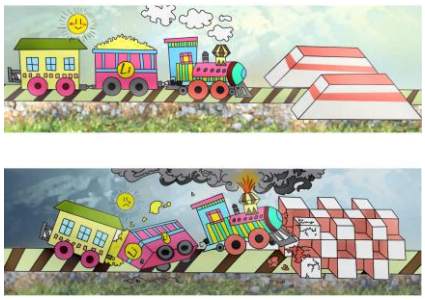

A new approach for using 2-carboxyethyl germanium sesquioxide (2-CEGS) as a replacement for GeO_2 in anodes for lithium-ion batteries has been proposed. Compared to GeO_2, having the 3D structure, 2-CEGS can formed 1D and 2D polymers, which facilitates the reversible penetration of lithium molecules into its structure. The lithium half-cells anodes based on 2-CEGS show a capacity up to 700 mA h g^{-1}, which is much higher than maximal theoretical capacity of graphite.